Dosimetry in Medical Physics

Advanced Lab Course Experiment at the Department of Medical Physics

by PD Dr. George Dedes and Dipl. Phys. Oliver Schmalz

November 12, 2024

1. Introduction

Dosimetry is an essential component of any workflow related to radioactivity. Two basic methods of dosimetry, often employed in Medical Physics, will be presented and used in this lab course.

The first method is film based dosimetry by means of radio-chromic films. The second method consists of measurements with a scintillation detector in a water phantom. Furthermore, a Monte-Carlo simulation tool will be used to predict dose distribution into the water phantom and measured by the scintillation detector.

Throughout the experiments a Strontium-90 (^{90}Sr) radiation source will be used. Such beta-emitting ^{90}Sr sources are usually employed in brachytherapy (from greek “near”), to treat certain types of cancer. Example applications of brachytherapy are cervical, breast and prostate cancers.

2. Personal Safety When Working With Radioactive Materials

For your own safety, please adhere to the three cardinal rules of radiation protection:

1. **Time** - As short as possible
2. **Distance** - As far away as possible
3. **Shielding** - As thick as necessary

Should any questions arise don't hesitate to contact your supervisor.

In case of emergency call the **TUM fire-department** under **112** (from the phone in room 143) or **089 289 112 (from your mobile)** and inform Dr. Thirolf in room 114, phone 14064.

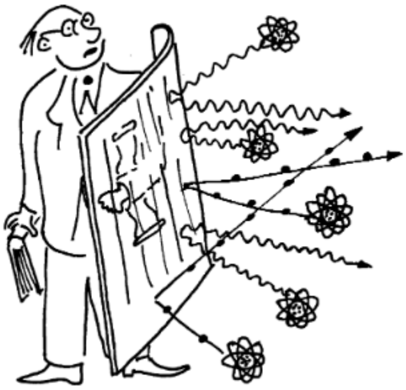

Figure 2.1.: Shield yourself

3. Physical Background

This chapter contains a summary of the basic concepts of radioactivity of interest to this lab course. In-depth presentation of the different types of ionizing radiation can be found in chapters 1 and 2 of [1] "Nuclear medicine physics: a handbook for teachers and students"[1]. A detailed dosimetry textbook (written in German) is [4], which is also available here.[2]

3.1. Radioactive Decay - Physical Quantities and Laws

Unstable nuclei undergo radioactive decay in order to transit to a lower energy state. There are several known paths of decay that alter the proton to neutron ratio of the nucleus in question. As a result, one or more particles are emitted, depending on the type of decay.

Another way for an excited nucleus to release excess energy is emitting photons. If these originate from the nucleus, they are called gamma rays (γ). Should they originate from atomic transitions (transitions of orbital electrons), they are called x-rays.

3.1.1. Relevant Formulas and SI-Units

3.1.1.1. Activity

The measurable quantity of nuclear decays is the *activity* A. It is defined as the "the average number of radioactive decays dN per time-interval dt":

$$A = \left\langle \frac{dN}{dt} \right\rangle ,$$

with the SI unit of activity being *Becquerel*, interpreted as one nuclear decay per second and expressed in dimensions of inverse second: $[A] = 1\,Bq = \frac{1}{s}$.

3.1.1.2. Law of Radioactive Decay

Since it is not possible to predict the exact moment when a specific nucleus will decay, one is restricted to describing the statistical behavior of an ensemble of unstable nuclei. Defining the *decay constant* λ as "the probability of the decay of a single radioactive nucleus per time unit" yields the *law of radioactive decay* in differential form:

---

[1] available at `http://www-pub.iaea.org/books/IAEABooks/10368/Nuclear-Medicine-Physics`

[2] `https://login.emedien.ub.uni-muenchen.de/login?url=http://dx.doi.org/10.1007/978-3-8348-2238-3`

$$-\frac{dN}{N} = \lambda dt, \tag{3.1}$$

where N is the number of unstable nuclei present at time t and dN the number of unstable nuclei that will decay in the infinitesimal time interval dt. The dimension of the decay constant is $[\lambda] = \frac{1}{s}$.

The solution of the differential equation 3.1 is

$$N(t) = N_0 e^{-\lambda t}. \tag{3.2}$$

with N_0 denoting the initial number of radioactive nuclei at time 0 and N_t the number of remaining radioactive nuclei after time t, assuming a decay constant λ.

This formula can be expressed in terms of activity A by using the relation $A = \lambda N$:

$$A(t) = A_0 e^{-\lambda t}. \tag{3.3}$$

3.1.1.3. Half-Life

An often used quantity characterizing specific radioactive isotopes is their *half-life* $T_{\frac{1}{2}}$. Considering an initial amount of isotopes N_0 in the law of radioactive decay, on average, there will be $\frac{N_0}{2}$ unstable nuclei left when $T_{\frac{1}{2}}$ has passed:

$$T_{\frac{1}{2}} = \frac{ln2}{\lambda}. \tag{3.4}$$

3.1.1.4. Mean Lifetime

By inverting the decay constant, one obtains the *mean lifetime* τ. It denotes the average time passing before an instable nucleus will decay:

$$\tau = \frac{1}{\lambda} = \frac{T_{\frac{1}{2}}}{ln\,2}. \tag{3.5}$$

3.1.1.5. Chain of Decays

Should the product of a radioactive decay be radioactive itself, then the whole process is known as a *decay chain*: isotope A decays into isotope B, increasing the number of B atoms present. These in turn produce isotope C while reducing the number of B.

The differential equation can be written as

$$\frac{dN_B}{dt} = -\lambda_B N_B + \lambda_A N_A(t_0) e^{-\lambda_A t}. \tag{3.6}$$

Solving this, we obtain

$$N_B = N_A(t_0) \frac{\lambda_A}{\lambda_B - \lambda_A} (e^{-\lambda_A t} - e^{-\lambda_B t}). \tag{3.7}$$

3.1.2. Radioactive Decay Processes

Nuclear Transmutations

What is defined as nuclear transmutations is the change in the composition of a nucleus. Thus the term is used to describe radioactive processes converting one element or isotope into another. There are several experimentally observed types of radioactive transmutation. In the following subsections, the main transmutation type of interest for this laboratory course is the beta decay. Nevertheless, a brief description of other nuclear transmutation types will be briefly mentioned.

3.1.2.1. Energetic Considerations

A quantity of high importance to all kinds of nuclear decays is the energy released by a radioactive decay, called *decay energy Q*. It is often given in units of *electron Volts* and is calculated by

$$Q = [(m(a_1) + \ldots + m(a_n)) - (m(b_1) + \ldots + m(b_m)] * c^2.$$

It expresses the rest mass difference between the parent (particles a_x) and daughter (particles b_x) atom. All natural (not induced) radioactive decay has a positive Q-value.

3.1.2.2. Alpha Decay

When a parent nucleus undergoes *Alpha Decay* a Helium nucleus called *alpha particle* (symbol α) is emitted.

$$\alpha =^4_2 He^{2+}. \tag{3.8}$$

The daughter nucleus has an atomic number and mass number are reduced by two and four respectively. The difference in binding energy before and after the decay is split between the products while maintaining conservation of momentum.

$${}^A_Z X_N \Longrightarrow^{A-4}_{Z-2} Y_{N-2} + \alpha + Q. \tag{3.9}$$

The released energy is virtually completely transfered to the alpha particle due to $m_N(Y) \gg m(\alpha)$, making the energy spectra of them discrete. Although experimental data shows some smearing of this discrete value, as the daughter nuclei do in practice gain some recoil momentum.

Natural alpha decay appears in nearly all elements with $Z \geq 82$. Below that border only induced alpha decays can occur, by providing enough energy, for example via photodisintegration (laser, high energy gamma- or x-rays) as well as bombardment with neutrons. A well known technical application is the use of thermal neutrons in nuclear fission reactors.

3.1.2.3. Beta Decay

The radioactive source of this lab course (^{90}Sr) decays via electron emission (beta decay) to Yttrium (^{90}Y), which in its turn decays again via beta decay to zirconium (^{90}Zr), with a decay rate of 99.9885%.

This kind of decay is caused by a surplus of neutrons in an unstable nucleus. Such a neutron can transform into a proton, a electron and an electron antineutrino:

$$n \Rightarrow p + e^{-} + \overline{\nu_e} + Q, \tag{3.10}$$

where Q is the energy released by this process. While the proton remains in the daughter nucleus, the electron and the antineutrino are emitted.

Considering the decay on an atomic scale shows that when the parent nucleus $^{A}_{Z}X_N$ decays, a daughter nucleus $^{A}_{Z+1}Y_{N-1}$ is produced:

$$^{A}_{Z}X_N \Longrightarrow ^{A}_{Z+1} Y_{N-1} + e^{-} + \overline{\nu_e} + Q. \tag{3.11}$$

Due to the kinetic energy being shared between the electron and the neutrino, the energy of the spectrum of the emitted electron is not discrete. Instead, it follows a distribution as shown in figure 3.1.

The average energy of the emitted electrons amounts to approximately $\langle E \rangle \approx \frac{1}{3} E_{max}$.

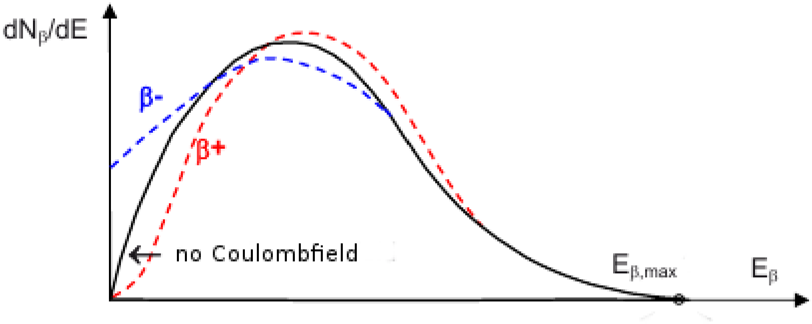

Figure 3.1.: Electron spectrum from beta decays. Blue-Dashed: Electrons with Coulomb Correction. Red-Dashed: Positrons with Coulomb Correction. Black: Without Coulomb Correction [4]

A *positive beta decay* (positron emission) is possible as well. Instead of surplus neutrons the nucleus carries an excessive amount of protons. This leads to the conversion of a proton into a neutron while emitting both a positron and an electron neutrino:

$$^{A}_{Z}X_N \Longrightarrow ^{A}_{Z-1} Y_{N+1} + e^{+} + \nu_e + Q. \tag{3.12}$$

Regarding the energy spectra of both positive and negative beta decay one needs to be aware of the Coulomb field of the nucleus produced after the decay. Repulsion or attraction respectively leads to differences in the spectra for both types of emitted electrons or positrons, see figure 3.1 on the previous page.

Radioactive Processes Without Transmutations

3.1.2.1. Gamma Decay

Gamma Decay is a mechanism for the deexcitations of a nucleus via the emission of a photon. The photon will carry the energy difference between the initial and final nucleus excitation state.

There is also the possibility to transfer that nuclear deexcitation energy to an orbital electron of the atom. This process is called *Internal Conversion.* Electrons ejected this way carry a kinetic energy that is the transition energy of the nucleus reduced by their binding energy B :

$$E_{e,kin} = \triangle E - B.$$

The orbital gap created can subsequently be filled by an electron from the outer shells, where the binding energy is lower. As long as there are electrons left in shells bound with less energy than at the position of the hole, further atomic transitions will occur. These atomic transitions to higher binding energy states causes the emittance of a *characteristic X-rays.*

3.2. Dosimetric Quantities

3.2.1. Effective Atomic Number

The *atomic number* Z represents the number of positive charges (protons) present in an atomic nucleus. The elements or isotopes of the periodic table are defined by the atomic number. To carry out calculations depending on Z for composites of different elements one needs an equivalent: the *effective atomic number* Z_{eff}, which expresses an average atomic number for non-monoelemental materials. In literature, there are several proposed approaches for its calculation, including weighted mass averages, power law type formulas with experimental exponents etc. For the purpose of our experiments we quote the calculation of [4], according to which human tissue, air, water and acrylic glass have an effective atomic numbers of about

$$Z_{eff} \approx 7. \tag{3.13}$$

Therefore, measurements of dose to water can be considered comparable to dose in human (soft) tissue.

3.2.2. Stopping Power

As *stopping power* we define the average energy loss per unit distance travelled by a charged particle in a medium. The total stopping power $\left(\frac{dE}{dx}\right)_{tot}$ can be splited in two terms.
One term for describes the energy loss $(\frac{dE}{dx})_{col}$ due to inelastic collisions of the charged incident particle with the target atomic electrons. The second term expresses the radiative energy losses $(\frac{dE}{dx})_{rad}$, due to *Bremsstrahlung.*

$$(\frac{dE}{dx})_{tot} = (\frac{dE}{dx})_{col} + (\frac{dE}{dx})_{rad}. \tag{3.14}$$

Collisional stopping power can be calculated using the famous Bethe-Bloch formula. For electrons it takes the following form:

$$S_{col} = (\frac{dE}{dx})_{col} = \rho \cdot 4\pi r_e^2 \cdot m_0 c^2 \cdot \frac{Z}{u \cdot A} \cdot z^2 \cdot \frac{1}{\beta^2} \cdot R_{col}(\beta). \tag{3.15}$$

Constants in this equation are the classical electron radius $r_e(= 2.818 * 10^{-15}\, m)$, the rest mass of the electron $m_0 c^2(= 0.511\, MeV)$, as well as the atomic mass unit $u(= 931,5\, MeV)$. The projectile's characteristics: the charge of the particle z and its speed v. For better readability, speed is given relative to the speed of light c: $\beta = \frac{v}{c}$. The residual function $R_{col}(\beta)$ is also dependent on the particle's speed and the ionization potential I of the material, plus higher order corrections. The characteristics of the absorber material Z, A and its density ρ complete the Bethe-Bloch-equation for electrons. The dimension of stopping power is energy loss per distance travelled, often quoted in $[S] = 1\,\frac{MeV}{cm}$.

3.2.2.1. Mass Stopping Power

Often the *mass stopping power* is used as a radiation related quantity. It takes into account the proportionality of stopping power and absorber density, making it approximately independent[3] of the absorber's density ρ:

$$\left(\frac{S}{\rho}\right)_{tot} = \left(\frac{S}{\rho}\right)_{col} + \left(\frac{S}{\rho}\right)_{rad}. \tag{3.16}$$

In literature the mass stopping power is expressed in units of energy divided by the mass dendity, usually given as $\left[\left(\frac{S}{\rho}\right)\right] = 1\,\frac{MeV*cm^2}{g}$.

---

[3] There is a minor dependency of the residual function $R_{col}(\beta)$ on ρ due to the so-called density effect which can be neglected for our experiments. Refer to [4]

3.2.2.2. Restricted Mass Stopping Power

For dose measurements though, not the (mass) stopping power is relevant, but the *restricted mass stopping power* $(\frac{S}{\rho})_{col,\Delta}$. The upper limit Δ of the energy considered is, by convention, given in units of eV and means that only events with energy losses below that limit are taken into account. This is due to the fact that the place, where an energy loss of the projectile occurs and the place that energy is absorbed by the target material are not necessarily the same. In dosimetry only the *locally* absorbed energy is relevant as a measurable quantity. Thus, bremsstrahlung and fast secondary particles, carrying the energy away from the place the initial event happened, are excluded.

For $\triangle \to \infty$ one obtains the *unrestricted mass stopping power*:

$$(\frac{S}{\rho})_{col,\triangle} \underset{\Delta\to\infty}{=} (\frac{S}{\rho})_{col}.$$

3.2.2.3. Linear Energy Transfer

Another important aspect when describing the energy transfer by ionizing radiation to a medium is the density of ionizations caused by a particular type of radiation. A way to describe this is the *Linear Energy Transfer (LET*, also commonly shortened to *L)*. It also makes use of the upper limit Δ and behaves quite similar to the collisional stopping power, although the definition is a bit different:

for charged particles of defined energy passing through matter the LET is defined as "the *average energy dE_L locally deposited* along the *track of length dl*":

$$LET = \frac{dE_L}{dl}, \tag{3.17}$$

LET does not include interactions which deposit energy non-locally, such as the emission of delta electrons or, in the case of electron and positrons, radiative energy losses.

Just like S_{col} the LET increases for lower kinetic energy of the incident particles. The SI-unit of the LET is $[LET] = [L] = 1\,\frac{J}{m}$, although it is more commonly given in terms of $\frac{keV}{\mu m}$.

LET is often used to indicate the ability of a certain type and quality of radiation to inflict serious damage to living cells. By the numerical value of LET, ionizing radiation can be categorized as densely or non densely ionizing. The DNA double helix strand has a typical size of a few nanometers. To cause potentially irrepairable damage to the DNA structure, double strand break has to take place. Therefore two or more events within a distance of a few nanometers are desired.

Figure 3.2a on the following page shows schematically the ionization density of different radiation types. Figure 3.2b on the next page shows a comparison of LET values of protons and electrons as a function of the particle energy.

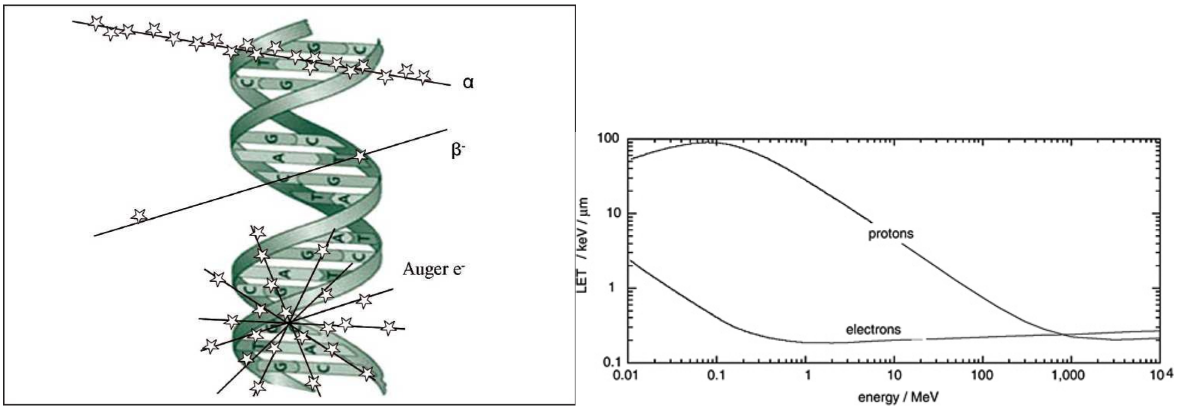

(a) A DNA double helix traversed by different particles. Each star marks an ionization event, schematically indicating the ionization density.

(b) LET for electrons and protons

Figure 3.2.: Linear Energy Transfer

3.2.3. Absorbed Dose

Absorbed dose D is the basic physical quantity used for radiological measurements. It is the energy deposited per unit of absorbing mass.

$$D = \frac{dE}{dm}. \tag{3.18}$$

The SI unit of absorbed dose is the Gray, which is defined as $[D] = 1\,Gy = 1\,\frac{J}{kg}$.

3.2.4. Equivalent Dose

The *equivalent dose* espresses the effect of absorbed dose on the human body, taking into account the different radiation qualities (particle types). A *weighting factor* w_R for the type of radiation is therefore introduced. The w_R for different qualities of radiation is based on experimental data, reflecting the discrepancies in biological effectiveness due to the differences in their LET[4]. Multiplying these weighting factors by the absorbed dose results in the *Equivalent Dose* H_T :

$$H_T = \sum_R w_R \cdot D_{T,R}. \tag{3.19}$$

Index T denotes the organ or tissue irradiated with the type of radiation given by the index R. Although the physical dimension is the same as for the absorbed dose, the SI unit *Sievert* (Sv) is used for equivalent dose to point out that it is a biological relevant quantity and not a purely physical one: $[H_T] = 1\,Sv = 1\,\frac{J}{kg}$.

Values for various types of radiation are given in table 3.1, while table 3.2 summarizes the dependence of the weighting factors on unrestricted LET values.

---

[4] among others, see ICRP 103 Appendix B or Krieger p. 320ff

Type of Radiation	Radiation Weighting Factor w_R
Photons	1
Electrons & Muons	1
Protons & charged Pions	2
Alpha Particles, Fission Fragments, Heavy Ions	20
Neutrons	Continuous Function of Neutron Energy

Table 3.1.: Radiation Weighting Factors

$L_\infty(\frac{keV}{\mu m})$ in water	$w_R(L)$
< 10	1
$10 - 100$	$0.32 * L - 2.2$
> 100	$\frac{300}{\sqrt{L}}$

Table 3.2.: Correlation of unrestricted LET L_∞ and weighting factors w_R

3.2.5. Effective Dose

The *effective dose* E takes into account the sensitivity of a given organ/tissue to the equivalent dose. The SI unit is again the Sievert to emphasize the biological meaning. The *tissue weighing factor* w_T is introduced to calculate E:

$$E = \sum_T w_T \cdot H_T. \tag{3.20}$$

Values of w_T for different organs are refined on a regular basis, the last time in 2007 in ICRP 103. See figure 3.3.

Tissue	w_T	$\sum w_T$
Bone-marrow (red), Colon, Lung, Stomach, Breast, Remainder Tissues	0.12	0.72
Gonads	0.08	0.08
Bladder, Oesophagus, Liver, Thyroid	0.04	0.16
Bone surface, Brain, Salivary glands, Skin	0.01	0.04

Table 3.3.: Tissue Weighting Factors (ICRP 103) w_T and sum over all tissues in the left column $\sum w_T$

4. Experimental Methods and Materials

The following sections will briefly describe the different methods and materials (detectors, calibration procedures, software tools) which will be used in the ensuing experiments. They also contain questions that should be answered during the experiment and documented in the report that will be submitted.

4.1. Strontium 90 (Sr-90)

For the purpose of this lab course, you will work with a pure beta-ray source made of Strontium-90 ($^{90}_{38}Sr$). The daughter nucleus after beta-decay is Yttrium-90 ($^{90}_{39}Y$).
When administered to the humans, both of these radioactive elements tend to concentrate in bones.[2], due to their chemical similarity to calcium[1].
As an artificial fission product, $^{90}_{38}Sr$ and its beta-decay product $^{90}_{39}Y$, almost the total amount of those isotopes found in the environment are man made. Sources of released material are nuclear weapon tests, nuclear events like Chernobyl (1984), as well as nuclear waste.

The decay chain is illustrated in figure4.1. There you can see that $^{90}_{38}Sr$ beta decays to $^{90}_{39}Y$ at a 100% decay rate. This, in turn, is transmuted into the stable Zirconium-90 ($^{90}_{40}Zr$). The main mode of decaying is by beta-decay again. In fact, the gamma-decay of Yttrium-90 is so rare, that it can be neglected. Table 4.1 on the following page lists the relevant data for both radioactive nuclei. Additionally, in 4.2 on the next page the energy spectra for both nuclei are shown, as well as the overall energy spectrum.

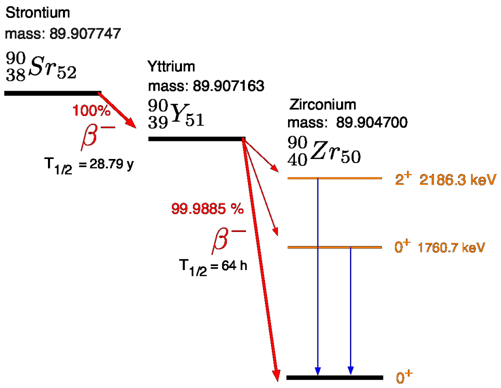

Figure 4.1.: Decay chain $^{90}_{38}Sr \rightarrow ^{90}_{39}Y \rightarrow ^{90}_{40}Zr$

In this experiment, the actual source is a small disc of diameter $d = 3\,mm$. It is made of a silver foil that has been injected with strontium carbonate. At the time of calibration in the year 2002 (exactly: at 9:47 a.m. on 11th May of 2002) the activity was $A = 33.3 \pm 10\%\,MBq$.

---

[1] Strontium and Calcium belong to the same group in the periodic table

Question 1: What is the activity A at the beginning of your experiments (t_{start})? Assume you will begin at 9 a.m.

Question 2: Using the calibrated activity and assuming that at the time of calibration t_0 the only source of activity was ${}^{90}_{38}Sr$. What number of Strontium-90 atoms have been present at t_0?

Sr-90			
$T_{\frac{1}{2}}$	$28.79 \pm 6\,a$		
β^-			
Avg. Energy [keV]	Max. Energy [keV]	Intensity [$\%$]	Daughter Level [keV]
195.8 ± 8	546.0 ± 14	100	0

Y-90			
$T_{\frac{1}{2}}$	$64 \pm 21\,h$		
β^-			
Avg. Energy [keV]	Max. Energy [keV]	Intensity [$\%$]	Daughter Level [keV]
25.0 ± 7	93.8 ± 16	$1.4E^{-6} \pm 3$	2186.282 ± 10
185.6 ± 10	519.4 ± 16	0.0115 ± 14	1760.72 ± 20
933.7 ± 12	2280.1 ± 16	99.9885 ± 14	0
γ			
2186.242 ± 25	2186.242 ± 25	$1.4E^{-6} \pm 3$	0

Table 4.1.: Decay of Sr-90 and Y-90. All ± signs in this table refer to the last valid digits.

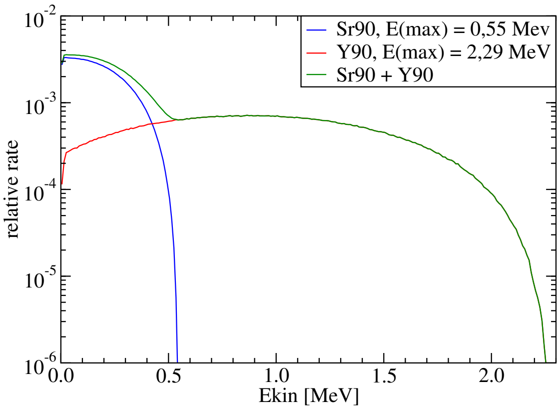

Figure 4.2.: Energy spectrum of Sr-90

Question 3: Making the same assumptions as before, calculate with respect to the total particle number at the time of calibration N_0
a)the percentage of ${}^{90}_{38}Sr$ atoms left,
b)the percentage of ${}^{90}_{39}Y$ present,
c)the percentage of ${}^{90}_{40}Zr$ present in the source at t_{start}

4.2. Radiation Detectors

There are several types of *radiation Detectors* in practical use, like ionization chambers, semi-conductor-based detectors and many others. In this experiment, an organic scintillation detector and gafchromic films are employed for measurements.

4.2.1. Scintillation Detectors

Scintillation detectors are based on the emittance of light after ionizing radiation has excited the detector's atoms or molecules. This is also known as *luminescence.* There are two types of luminescence, called *phosphorescence* and *fluorescence.* Phosphorescence means emittance with a time-delay (about $10^{-3} - 10^{2}\,s$), while with fluorescence photons are emitted instantly after excitation ($10^{-9} - 10^{-7}\,s$). Both types of detectors are widely used in practice. They are available in liquid, solid and even gaseous forms.

The emitted light is transferred through glass fibers to a photomultiplier. There, the light coming from the scintillator is converted to an electrical current by utilizing the photoelectric effect. Subsequently this current is amplified measured by the attached counting device.

In general, the characteristic properties of scintillation detectors are different for each type of ionizing radiation. The most important properties determining their quality and applications are:

- Conversion by fluorescence or phosphorescence
- State of matter
- Self-transparency for the emitted wavelengths
- Compatible indexes of refraction for coupling them with glass fibers
- Efficiency in converting the incident radiation energy to a flux of photons
- Linearity of conversion

4.2.1.1. Fluorescence Detectors

Fluorescence detectors provide almost real-time measurement of the impinging irradiation, due to their short emission times. One can distinguish them in inorganic and organic types.

The inorganic scintillators can only be manufactured from crystals, since their properties are governed by their crystalline structure and added impurities. Within these structures, energy bands exist, determining what quanta of energy can be absorbed and in what way such a high-energy state can be deexcited again. Inorganic scintillators generally are made of high-Z materials, increasing their sensitivity to gamma-rays.

Organic scintillators use a different approach. They are based on aromatic hydrocarbon molecules (low-Z) either disolved in a liquid or a plastic compound that provides a solid structure. It's the molecules themselves that are centers of fluorescence activity and not the underlying crystallic structure.

4.2.1.2. Organic Scintillators

The plastics serving as solvent for organic scintillation molecules can be manufactured to be water-equivalent, i.e. $Z \approx 7$. This means that the dose measured with these organic scintillators is comparable to the dose that would be deposited in human soft tissue. In addition, the conversion speed of incident radiation to emitted as light is in the scale of nanoseconds. Transparency to the emitted photons is, in contrast to inorganic crystals, no issue with these devices, see figure 4.3.

Disadvantages in comparison to inorganic scintillation crystals are the low scintillation efficiency, i.e. low light output, as well as their lower sensitivity to gamma-ray energies below $100\,keV$. To compensate for the low light output, a good photomultiplier is required, while sensitivity to incident photons increases increasing the thickness.

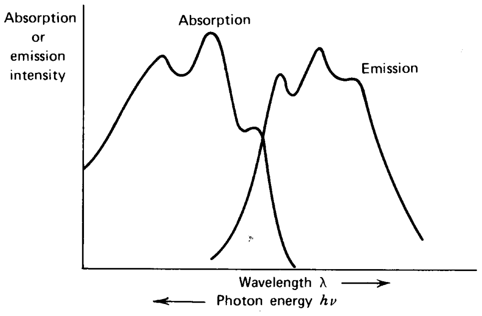

Figure 4.3.: Absorption and emission spectra of a typical organic scintillator

4.2.1.3. Optidos^{TM}-system

The Optidos™ scintillation detector system by PTW Freiburg[2] has been designed for the purpose of quality assurance and dose verification in brachytherapy. It features an organic scintillation detector made of water-equivalent plastics with increased sensitivity for low energy photons and very good linearity for electrons. A radioactive check source

---

[2] `https://www.ptw.de`

is available and will be used in order to compensate for the decrease in detector sensitivity over time and for other environmental factors.

The detection system consists of four parts:

1. Scintillation detector Type 60006 with a glass fiber attached
2. Optidos dosimeter Type 10013
3. Check source (Sr-90)

4.2.1.4. Scintillation detector Type 60006

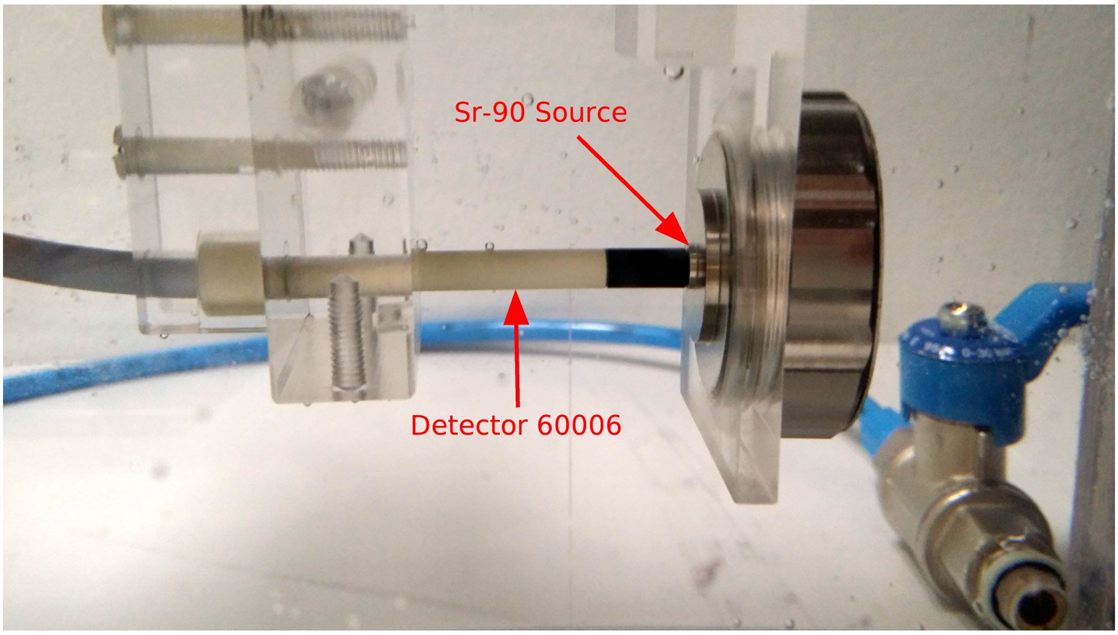

Figure 4.4.: Detector Type 60006 with check source in water phantom

The scintillation detector Type 60006 contains a cylindrical standard organic scintillator[3] with a diameter of $1\,mm$ and a height of $1\,mm$. The active detection volume amounts to $0.8\,mm^3$. It sits $0.4\,mm$ behind the front edge of the detector assembly. Figure 4.5 on the next page shows the result of a Monte Carlo simulation of the detector tip in water, simulating electrons[4] of up to $3\,MeV$. The color bar shows the comparison of the deposited dose in the detector material to that deposited in water. For each material marked in the figure, the corresponding density is denoted next to its name. As it becomes apparent in the figure, close to the organic scintillator there is no major difference

---

[3] One of the most commonly used organic scintillators: The Bicron Corp. "BC-400"

[4] The manufacturer of the scintillation crystal actually states a correction factor of 1.03 for readings from a Sr-90 source due to minor deviations from linearity in event-to-light conversion for low-energy electrons. This is already taken into account during calibration

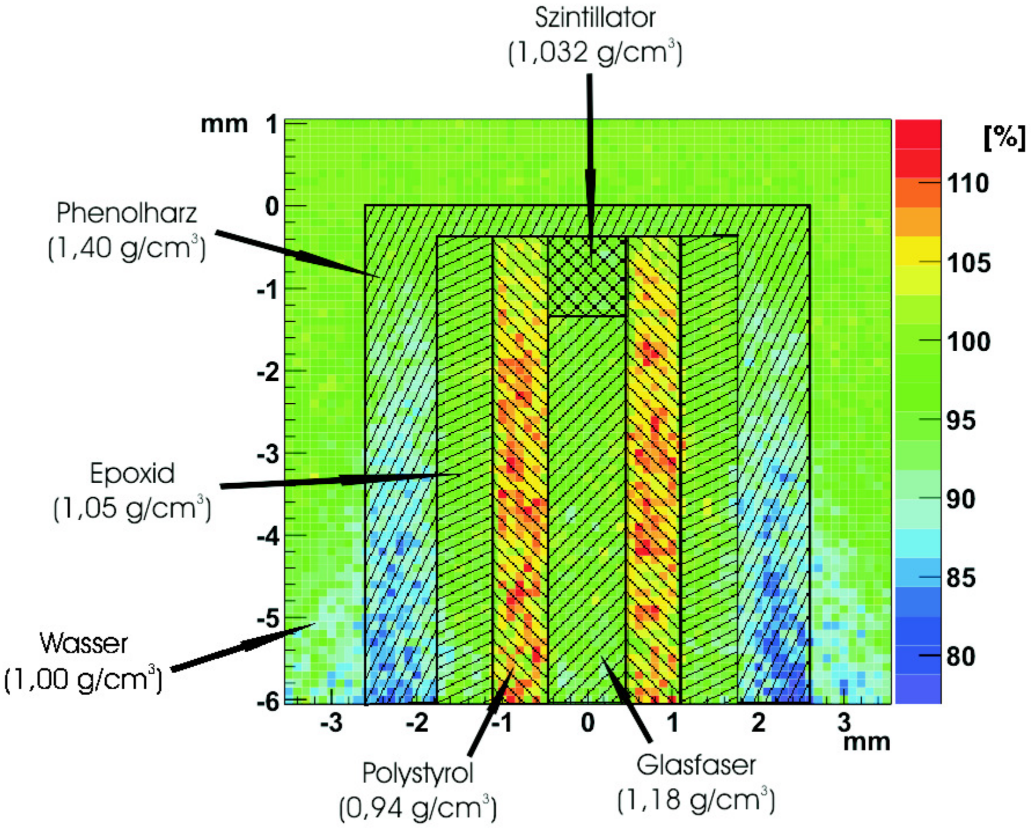

Figure 4.5.: Geant4-simulation of dose deposited in the scintillator Type 60006 compared to the dose that would be deposited in water. Dose to water = 100%

in deposited dose with respect to water. Behind it though, the denser phenol resin as well as the less dense polystyrene display larger discrepancies. Therefore, it is recommended to point the tip of the scintillator towards the source during the measurements.

4.2.1.5. Optidos dosimeter Type 10013

When light enters the dosimeter through the glass fiber, a photomultiplier converts it to electrical current and amplifies it. This means that the Optidos Type 10013 device does not count single events, but measures the stream of photons. As a result the maximum accuracy of 0.5% can only be provided down to a lower dose rate limit of $\overset{\circ}{D} = 0.4\,\frac{mGy}{s}$. The upper limit for precise measurements is $\overset{\circ}{D} = 0.4\,\frac{Gy}{s}$. At this point the photomultiplier is saturated.

Preceding any measurements, the dosimeter has to be calibrated to obtain the absolute dose deposited in water. To compensate for deviations in environmental variables and background radiation, as well as for the aging process of the device, it is mandatory to determine a correction factor before performing measurements. For the calibration procedure a ^{90}Sr check source is utilized:

1. A basic calibration is performed every two years by the manufacturer. During this procedure, the *displayed check value* $k_{p,0}$ is determined. $k_{p,0}$ is the dose-rate $\overset{\circ}{D}$ in units of $\frac{Gy}{min}$ displayed by the Optidos device after irradiation for $60\,s$ using the check-source. The most recent Certificate of Calibration[5], i.e. the documentation of the last calibration, can be found in the laboratory. Before your measurements, you have to calculate k_p from this by applying the law of radioactive decay on the source (see equation 3.2 on page 5)
2. To compensate for environmental variables affecting the measurements, you have to perform a gauging. This is achieved by first performing a test-run for $60\,s$ without any source of radiation. The value displayed by the Optidos device should be less than $0.5\% \cdot k_{p,0}$.
3. Subsequently another measurement k_m is performed with the check source, also for $60\,s$. The result of this measurement is the *correction factor* k_p/k_m. In the calibration relation used by the software of the Optidos device, k_p/k_m is used to account for different measurement conditions in comparison to those during basic calibration.

Based on the aforementioned procedure, the calibration relation to transform the measurement displayed by the Optidos to dose to water is:

$$D_W = k_Q * \frac{k_p}{k_m} * N_W * M. \quad (4.1)$$

D_W : dose to water

k_Q : correction factor for beam quality (type and energy of radiation, $k_{Q,Sr90} = 1.03$)

k_p : expected displayed check reading after $60\,s$ of irradiation

k_m : measured value after $60\,s$ of irradiation with the check source

N_W : calibration factor for dose to water ($=$ 1)

M : displayed value

Question 4: Using $k_{p,0}$, calculate the expected k_p on the day of your experiment.

Values (Detector Serial-Number: 000058, Optidos Serial-Number: 000037):

- Date of calibration: 13. October 2015
- $k_{p,0} = 1171.0\,\frac{mGy}{min}$
- $T_{\frac{1}{2}}(^{90}Sr) = 28.79\,y$

---

[5] “Kalibrierschein”

Software (LabView)

For automated measurements at multiple points in space defined by a raster (*grid-scans*) with the Optidos you will use a software called "Optidos_Gridscan". It is written in LabView (National Instruments), a graphical programming language commonly used for measurement and automation tasks. In LabView, programs and sub-routines are referred to as *virtual instruments* (VIs). Optidos_Gridscan includes, among others, VIs for serial communication with the Optidos device and controlling of the three-axis stepping motor stage. It brings them together in a GUI, enabling you to perform automated grid-scans for dose measurements in three dimensional space.

It also includes a simple implementation for visualization of the acquired scans. This allows the user to quickly estimate the center of the source measured in terms of detector position variables.

4.2.2. Radiochromic Films

Radiochromic films (RCF), also referred to as Gafchromic, the trademark of the main manufacturer Ashland, are used in radiation therapy and treatment planning since 1984. Originally limited to high-dose applications like treatment of food packaging and sterilization of medical equipment, RCF have become popular since the emergence of the EBT[6] type films by Ashland in 2005, as these provide clinically relevant dose ranges (EBT 1: $0.01 - 8\,Gy$). As the main requirement for their usage is a good scanning device with transmission mode capability, they pose an affordable alternative to other detector systems. The sheets of EBT film are flexible, can be cut to the desired size and are able to withstand water for several hours. In comparison to radiographic films (comparable to old photographic films), they neither need to be stored in dark rooms, nor must they be developed using chemicals. As they are self-developing, they provide a convenient way of *Quality Assurance* (QA) in treatment planning. Their main application in clinical routine is the verification of treatment plan conformity of radiation treatments with high dose gradients.

The main part of a radiochromic film is its *active layer*. It is a thin coating of a radiosensitive chemical substance, which is enveloped between two protective layers. These layers, usually made of transparent plastics, keep the active layer in place and may well provide and improve other aspects of the whole film structure, like stability, flexibility, water resistance, etc., that generally improve the handling of RCF.
The active layer changes color as consequence of exposure to ionizing radiation[7]. In general, it is based on crystalline polyacetylenes. Figure 4.8 shows a schematic representation of a modern active layer.

The underlying physical process is the polymerization of the diacetylene monomers into acetylene polymers, meaning that the rod-like monomers form intra-molecular bonds (i.e. they polymerize). These bonds cause the initially optically transparent active layer

---

[6] *E*xternal *B*eam *T*herapy

[7] heating and UV light have the same effects, but in modern films the other layers provide good protection against them

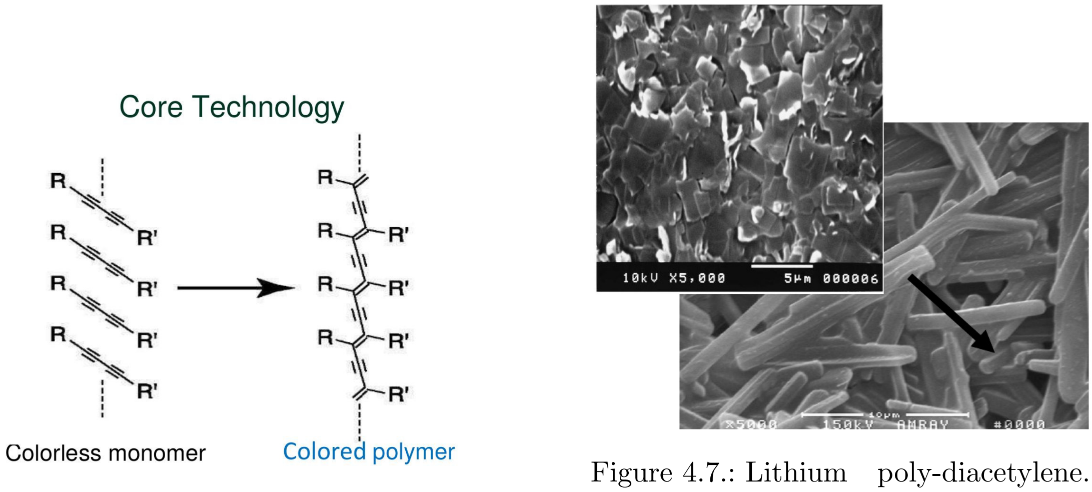

Figure 4.6.: Schematic of the polymerization

Figure 4.7.: Lithium poly-diacetylene. Each "rod" is a single molecule

Figure 4.8.: Poly-diacetylene

to acquire a characteristic blue color, since light absorption in the visible spectrum is increased. This is especially true for the red wavelengths[8].

The highest exposure, the longer these polymer chains become, causing an intenserer coloring of the film. What the human eye interprets as darkening and intenser color, can physically be described using the *optical density* OD,

$$OD = \log \frac{1}{T}. \tag{4.2}$$

it is the logarithm of the inverse *transmitted intensity* T. A scanning device with a transmission unit will use its (white) source of light to acquire values of transmitted intensity. An increased optical density means that less light will be transmitted through the film.

During the process of scanning, each small area measured is assigned a value. These small quadratic areas over which the scanner's CCD-chip measurements are averaged, are called *pixels*. Scanning a radiochromic film will thus provide a matrix of pixel values with a constant pixel size given in units of *dpi* (dots per inch[9]).

Pixel values may be given in terms of RGB values. In pictures scanned with a color depth of forty eight bit, each of the *R*ed, *G*reen and *B*lue channels can assume values ranging from 0 up to 2^{16} (= 16 bit), ranging from no transmission to full transmission:

---

[8] maximum absorption for EBT-type films is around 633 nm, see figure 4.9

[9]
$$1\,in = 2.54\,cm$$

$$0 \leq \begin{array}{c} \mathit{Red} \\ \mathit{Green} \\ \mathit{Blue} \end{array} \mathit{color\ value} \leq 2^{16} = 65535.$$

To measure the effect of irradiation on radiochromic films, the pixel values of irradiated films need to be compared to the pixel values of not irradiated ones from the same production batch (lot number). Introducing the effective optical density *netOD*, the difference in optical density before and after exposure,

$$netOD = OD_{irr} - OD_{not} = -\log\left(\frac{PV_{irr}}{PV_{not}}\right). \tag{4.3}$$

The indexes stand for (*not*) *irr*adiated and PV is used as abbreviation for pixel value.

Having calculated the value of netOD, only one more step is necessary to acquire the desired *dose* values from measurements with radiochromic films. The reaction of the films to the energy deposited needs to be calibrated. At the chair for experimental medical physics this is usually done by irradiating films of the same type and production date ("lot number") at a linear accelerator while using an ionization chamber as a dose reference during the irradiation of the calibration films. After that procedure, the netOD is correlated to the measured dose and a calibration curve is fitted to the values.

Depending on the dose delivered it is feasible to use only one (the red) or all three of the RGB color channels. Dose measurements that will be performed in this lab course can be restricted to the red channel, as recent literature states up to $20\,Gy$ as upper limits for single channel dosimetry.

A very important aspect to be mentioned is the averaging nature of radiochromic films. Various studies have shown that films of the EBT type are very precise dosimeters for absolute doses under the premises of homogeneous fields irradiating large enough pieces of film. This comes from fact that for absolute dose measurements one chooses large regions of interest (ROI) to analyze in a piece of film. Analysis is then done by creating a histogram including as many pixels as possible avoiding the edges of the film, as well as the boundaries of the irradiation field. An example from clinical practice would be pieces of 4 by 5 cm irradiated by a linear accelerator with a field size of 10 by 10 cm. Assuming the films are scanned with a resolution of $150\,dpi$, the length of a pixel amounts to $0.169\,mm$. A typical region of interest in this case might be 2.5 by $2.5\,cm$ which would include more than $2 \cdot 10^4\,pixels$. Averaging over such a number of single measurements in a homogeneous field would yield very stable mean values from a statistical point of view.

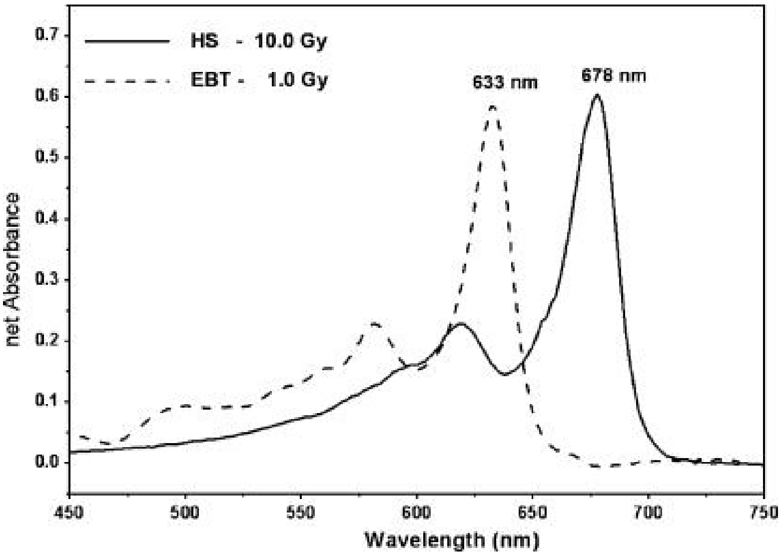

Figure 4.9.: netAbsorbance for EBT and the older HS radiochromic films. Note the tenfold increase in sensitivity of EBT over HS[3].

The general characteristics/advantages of radiochromic film dosimetry in comparison to other methods are:

- 2D-dose measurement
- high spatial resolution
- linear dose and energy dependence
- water equivalence
- low technical requirements (scanner)
- easy handling
- only one calibration needed per lot

4.3. Monte Carlo simulation

Monte Carlo simulation of particle interactions with matter are computer algorithms based on the random sampling from known probability distributions on the microscopic scale to obtain macroscopic results, e.g. interactions of electrons with matter to obtain the macroscopic quantity of dose deposited in water.

Monte Carlo algorithms are commonly used to accurately simulate experiments that are either difficult/not possible to be repeatedly performed (ie dose calculations in patients) or to predict physical quantities before the actual experiment (ie radation protection calculations for shielding design of large facilities). Accurate physical models and detailed look-up tables of experimental data are required, in order to reliably reproduce complex physical processes.

The following is a general scheme of Monte Carlo Experiments in physics, performed for every single particle simulated:

1. Select a particle coming out of the source to be simulated
2. Sample from total cross section distributions to determine the distance to the next interaction (step length)
3. Determine the type of interaction by sampling from partial cross section distributions
4. Determine if there is a secondary particle produced by the interaction. If yes, define its properties (direction, energy, momentum etc) by sampling from the appropriate distributions and update the properties of the initial particle (direction, energy, momentum etc)
5. Repeat steps 1-4 until all particles have been absorbed, have their energy dropped below a certain threshold or come at rest, or have left the area of simulation

4.3.1. FLUKA & FLAIR

In the context of this lab course FLUKA[10](FLUktuierende KAskade) will be used for simulating our experiment in the water tank. FLUKA is written in Fortran[11]. By using a GUI for FLUKA called FLAIR[12] (FLUKA Advanced Interface), the necessary simulations can be performed without the need to code in Fortran.

The FLUKA software can be used without FLAIR too. All input parameters to the simulation are provided in the form of the so-called data cards separated by delimiters[13]. This method is very cumbersome and error prone. Therefore, the graphical user-interface FLAIR will be used for the purposes of this lab course. The input file is still based on the aforementioned cards, but FLAIR is automatically creating, starting from the user specified options defined in the graphical interface (filling of predefined fields, choosing options from drop-down menus etc).

In general, the input file contains three different types of information:

1. Source/particle information. This usually defines the type of source particles, their kinematic distributions, the number of particles (primaries) to be simulated, etc
2. Geometrical and material descriptions. This usually includes volumes (rectangular water tank), positions and materials (water, plexiglass etc)

---

[10] http://www.fluka.org/fluka.php

[11] Note that Fortran can only handle names of up to 8 letters/digits length

[12] http://www.fluka.org/FLUKA/flair/

[13] e.g. spaces

3. Cards defining the scorers. The latter record the required information (ie 3D dose distrubution)

There is an input file prepared for you. All parameters are set to resemble your real experiment performed in the water tank. The only required mofifications concern the USRBINs (volumes of scoring dose to water) and they will be described in the next chapter. Note that FLUKA results are always reflects normalized per primary particle and dose is expressed in GeV/g.

A set of 6 videos which can be found in the lab course web page explain in detail how to use FLUKA via FLAIR:

https://drive.google.com/drive/folders/1gEaM6M52-GazdmNVriR1hRwy7lqmEwLG?usp=sharing

Please watch them prior to the lab course appointment.

5. Experimental Procedure

5.1. Summary

Keep a detailed record of all the steps and measurements in the lab. This will allow you to trace back any sources of errors/problems and it will be the basis of the report you will have to submit for your evaluation.

The aim of this experiment is to acquire the necessary measurements and to compare them with the results of the FLUKA simulations. The comparison will be done on the basis of two sets of measurements. The first is a high-statistics, high spatial resolution 1D profile of the dose vs the distance from the source, along the central axis of the cylindrical source. This will be from now and on called the longitudinal dose profile. The second set of measurements consists of two-dimensional scans of the dose, on planes perpendicular to the central axis of the source. These measurements will be called lateral dose measurements.

The proposed experimental steps are the following (red for the film experiment, blue for the Optidos/scintillator experiment and black for generic steps) and they will be detailed in the coming pages:

1. Make sure that Optidos is powered on
2. Prepare the film-stack
3. Irradiate the film-stack
4. Calibrate Optidos
5. Prepare the scintillator detector set-up for measurements in water
6. Find the coordinates of the center of the source
7. Find how far the dose extends longitudinally
8. Find how far the dose extends laterally
9. Start a long OPTIDOS scan to obtain a high resolution longitudinal depth profile
10. Start a long OPTIDOS scan to obtain 3-4 lateral plane grid measurements
11. Simulate the Optidos measurements with FLUKA
12. Calculate your calibration curve for the gafchromic films with Matlab

13. Scan the films
14. Use Matlab to extract histograms/profiles from the digitized films
15. Perform the analysis (to be completed at home)
16. Write a comprehensive report (to be completed at home)

5.2. Grid Scans Using the Optidos Device

Note: The Optidos device should be switched on at least 30 minutes before the calibration procedure is started!

Never bend the optical fiber with a radius less than 10cm!

Instruction 1 Starting LabView

1. Log into the OPTIDOS-workstation using the log-in credentials at the computer,
2. Navigate to 'Y:\project\prakt-dosimetry\Work\Groups' (Shortcut on the Desktop),
3. Create a folder with your last names. You will save all your data here!
4. Go to 'Y:\project\prakt-dosimetry\Work\Software\LabView',
5. Run the 'Optidos_Gridscan.exe'.

The GUI of the VI will open (see figure 5.1 on the next page).

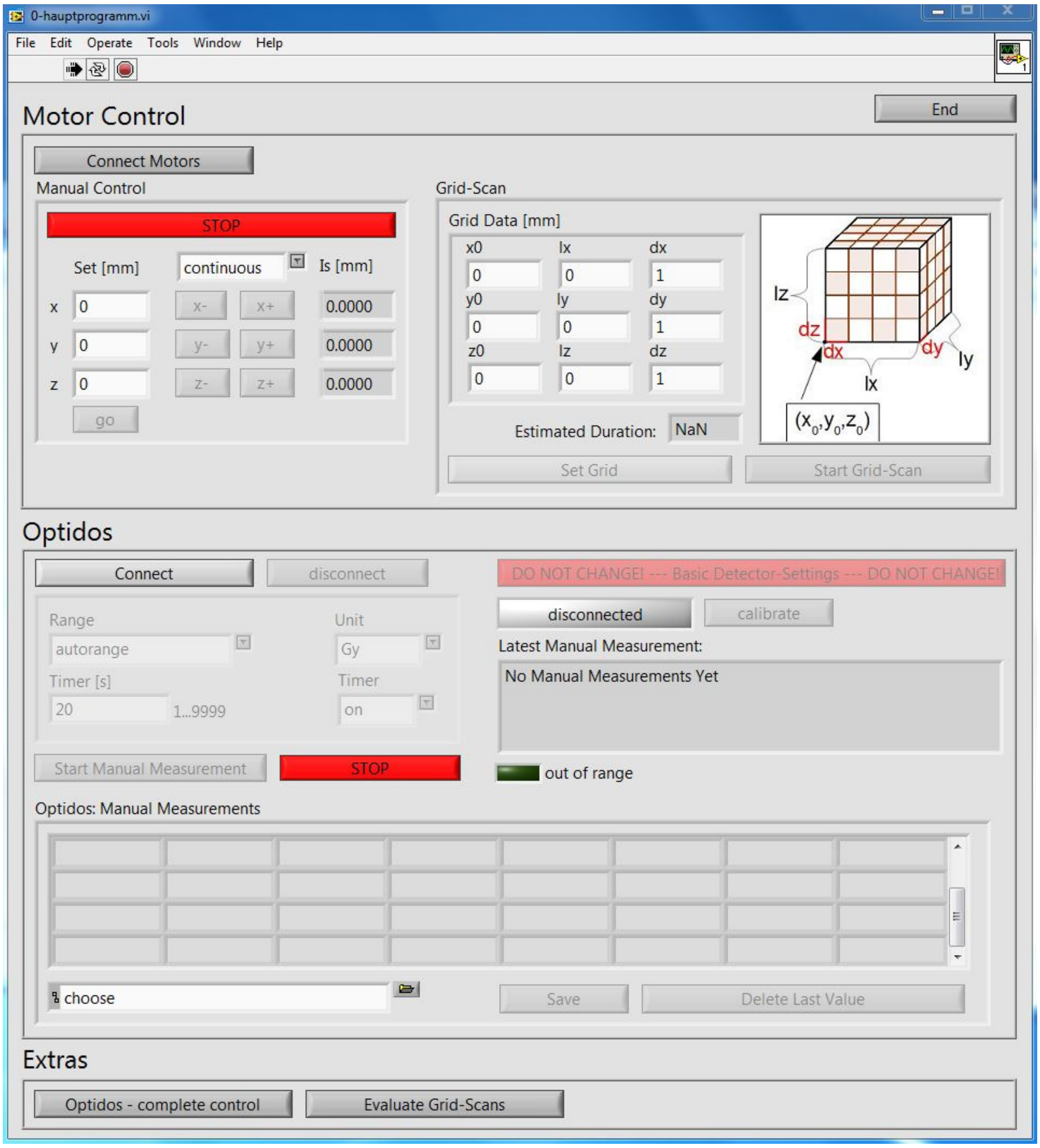

Set [mm]: continuous
Is [mm]

	Set [mm]	Is [mm]
x	0	0.0000
y	0	0.0000
z	0	0.0000

Grid Data [mm]

x0	lx	dx
0	0	1
y0	**ly**	**dy**
0	0	1
z0	**lz**	**dz**
0	0	1

Estimated Duration: NaN

Range: autorange
Unit: Gy
Timer [s]: 20 1...9999
Timer: on

Latest Manual Measurement:
No Manual Measurements Yet

choose

Figure 5.1.: OptidosGrid-VI

To calibrate the Optidos, you have to measure the background and then determine the value of k_m.

Instruction 2 Calibrating the Optidos Device

Everything related to the Optidos detector system is organized in the tab labeled Optidos.

1. Click Connect (1) to connect to the system.
2. The calibration process is started by clicking calibrate (2).
3. What is your calculated value of k_p?
   Click OK.
4. Follow the on-screen instructions. They appear in a yellow box at the bottom of the screen.

You need to call your supervisor during the calibration procedure. He has to put the check source into the plastic holder.

Use the acrylic walls to protect yourself from radiation!

When the calibration is done you have to change the set-up. Let your supervisor remove the check source from the plastic holder. He will then mount the second ^{90}Sr on the experimental setup and put it in the water tank.

Instruction 3 Preparing Optidos Measurements

1. Close the drain at the bottom, then fill the water tank,
2. Put the motor-stage on top of it,
3. Mount the scintillator on the experimental setup,

When everything is put together you can perform your first test run.

Instruction 4 Task: Find the Central Axis of the Source

---

1. In the field called Motor Control click Connect Motors and wait for the stage to self-adjust,
2. Validate the directions by using the directional buttons,
3. Start a 10 second manual measurement for testing purposes, by clicking Start Manual Measurement,
4. The next step is to work with a grid scan. In the upper right corner there's the tab called Grid-Scan. Refer to the pictured cube on the following page for an explanation of the variables. "Estimated Duration" will show you the estimated time of the measurement,
5. Now try to move the scintillator as close to the center of the source as possible by visual guidance, using the Manual Control. This will give you a first estimate of the central axis location, denoted here as $(v_{x0}, v_{y0}, 0)$
6. In Optidos set the "Timer" to 5 seconds,
7. Then make 2D grid scan to find more accurately the source center. For that measurement please use the $(v_{x0}, v_{y0}, 0)$ as initial guess and make a scan around it covering $10\,mm$ of l_x, l_y, at $0.5\,mm$ steps: center:

$$\begin{array}{ccc} x_0 & l_x & d_x \\ v_{x0} & 10 & 0.5 \\ y_0 & l_y & d_y \\ v_{y0} & 10 & 0.5 \\ z_0 & l_z & d_x \\ 0 & 0 & 0 \end{array} \tag{5.1}$$

8. Start the grid-scan by hitting Set Grid, followed by Start Grid-Scan.
9. When the scan is finished you have to choose a .txt-file to save the recorded data. Do this by clicking the folder-icon on the bottom of the screen, enter a filename and finish by clicking Save.
10. To evaluate the measurement click Evaluate Grid-Scans at the bottom of the VIs front panel.
11. Load the recently created text file and use the "Profile" tab on the right hand side to inspect the profiles of your scan.
12. Repeat the whole procedure (steps 7 to 11 with improved grid-scan values) until you're satisfied with the precision.
13. Note down the source center coordinates as you will need it for the subsequent measurements!

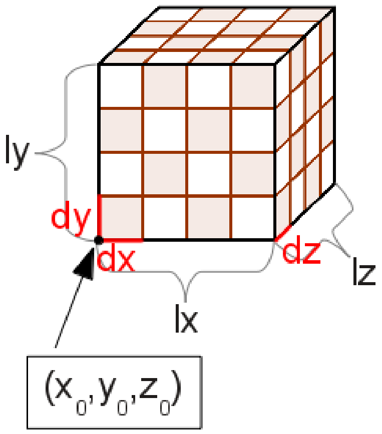

Figure 5.2: Grid-Scan legend (cube)
x_0 : starting coordinate
dx : step-length in x-direction
lx : path-length in x-direction
Check if the axes are the same for your experiment!

After finding the central axis of the source, you will perform a few measurements, in order to obtain the longitudinal depth profile. This will allow you to identify how far the dose extends longitudinally.

Instruction 5 Longitudinal Dose Measurements

1. Use the source center coordinates as x_0 and y_0.
2. Do a first longitudinal (1D) scan, covering a large l_z range (you need to decide how much) with large d_z steps.
3. Start the grid-scan by hitting Set Grid then followed by Start Grid-Scan.
4. Save the scan.
5. Evaluate the scan by clicking Evaluate Grid-Scans and decide up to which z and with what d_z step you will do a high resolution lognitudinal depth measurement.
6. Perform the high resolution longitudinal measurement of approximately 15 min, by setting the appropriate grid parameters Set Grid then followed by Start Grid-Scan.
7. Save the scan.
8. Verify that the scan is meaningful by clicking Evaluate Grid-Scans.

The last set of measurements aims at obtaining the lateral dose planes. You will need again to first make a rough measurement that will help you identifying the appropriate parameters, followed by a longer high-resolution measurement.

Instruction 6 Lateral Dose Measurements

1. Use some of the 2D measurements you made in order to find the source center, or make new ones that will allow you to identify how far the dose extends lateraly. These should be of short duration with coarse d_x, d_y and large l_x, l_y
2. Start any new scans by hitting Set Grid then followed by Start Grid-Scan.
3. Save any new scans.
4. Evaluate the scans by clicking Evaluate Grid-Scans and decide up to which x and y and with what d_x and d_y steps you will do high resolution lateral dose measurements.
5. The final high-resolution lateral scan should take approximately 1 h.
6. Set the grid-scan as a 3D grid by hitting Set Grid. The z dimension should be set such that the lateral measurement is performed at 2-3 different depths.
7. Save the scan.
8. Verify that the scan is meaningful by clicking Evaluate Grid-Scans.

The required set of measurements is now complete and with that you can perform the data analysis described in section 6 (Data Analysis and Report).

5.3. FLUKA-Simulation

While the Optidos acquires the long lateral grid-scan, you will simulate the expected dose distribution using the Monte Carlo code of FLUKA.

To do this, you first have to connect to a Linux workstation. On the desktop you will see an item called “FLUKA.rdp”. Double-clicking it initiates the remote desktop connection[1] to a Linux workstation. Use the same login credentials as you did for Windows and check that the module “sesman-Xvnc” is used.

Accessing FLAIR is done via console. Use the shortcut to “console” on your Linux desktop and enter “flair”. Now you should see the main window. As shown in the video tutorials, click “Open” and load the file “praktikum.flair” you can find in the “Software/Fluka” folder. In the top menu bar you can take a look at “Input” and “Geometry” to see the actual set-up. After inspecting those two tabs please return to the main tab. The simulated geometry consists of a Sr-90-source in water, which is confined in an acrylic case without lid. The so-called water phantom is placed in air and to keep it in line with FLUKAs demands the sphere of air is surrounded by a big “black hole”[2]. So the simulated environment is pretty similar to your real-life experiment.

Before running the simulation, please save your personal version of the project by using “Save” and creating a new “*.flair” file in your Groups directory.

Now you can run a test simulation with 10000 decays. After the simulation finishes, you can process the data and plot the longitudinal and lateral profiles, as shown in the video tutorials. Note that the longitudinal dimension z in the Optidos scan is the dimension x in FLUKA. Another important detail is that, contrary to the Optidos scan which registers dose in Gy within a certain time in sec, the dose in FLUKA is scored as $GeV/(gr \cdot N_{decays})$.

Question 5: How do you compare the simulated dose to the measured dose, in units of Gy/sec?

The next step is to adjust some of the FLUKA parameters accordingly and launch a long simulation.

---

[1] Hint: To switch between full-screen and windowed mode use CTRL + ALT + ENTER

[2] the black hole is used to destroy particles leaving the volume of interest for simulation.

Instruction 7 FLUKA Simulation

1. Adjust the two so-called USRBIN scorers. Try to replicate your measurements with the Optidos by implementing similar grid parameters.
2. Launch a test simulation of 100000 decays. Observe the time per primary and note its value.
3. Plot the different distributions in FLAIR to verify that the previously chosen grid parameters are meanignful
4. Using the time per primary, estimate the number of decays that can be simulated in about 40 min
5. Launch as simulation with that number of decays.

When the simulation is done, look at the tab “Data”. You can process the data as shown in the video tutorials (by clicking “Process”). For your analysis at home, you need to convert the binary “*.bnn” file to text files. For every “*.bnn” file hit the “Convert file to Ascii”-button and a file named *.bnn.lis will be created. This is the text file you will need for your analysis. You can briefly inspect it with the FLAIR editor.

6. Data Analysis and Report

6.1. Required Data

To perform the analysis make sure that have acquired at least the following data:

- Measurement: A txt-file for each the coarse and the high-resolution longitudinal dose profile.
- Measurement: A txt-file for the 3D scan of the high-resolution lateral dose measurements.
- Simulation: A .lis file for each of the two USRBIN scorers

6.2. Obtaining Absolute Dose

As mentioned in the simulation section, the dose in FLUKA is scored in units of $GeV/(gr \cdot N_{decays})$, while in the measurement as Gy in a given time interval. You will need to convert both to Gy/sec. For the measurement this is trivial. For the simulation, you will need to use the activity of the source to perform the conversion. From this point and on, any absolute dose comparison should be presented in Gy/sec.

6.3. Analysis

For the analysis of the data (in the form of text files), you can use the programming language of your choice (Python, R, Matlab, C, etc). The measured data contain a few header lines. After that the data are arranged in a line per point of measurement according to *x[mm] y[mm] z[mm] Value Resolution Range*. *Value* indicates the dose measured in the time duration of the measurement. *Resolution* indicates the error in %. Finally *Range* indicates the detection mode and can be ignored. When plotting the measured data, please plot the error bars too. This is not required for the simulations.

The text files from the simulated data contain a header. The header describes the number of bins in each dimension, the bin width in cm and the structure of the recorded data. After the header, the dose measurements in every voxel/bin are listed in a structure of 10 columns and as many lines required. The first data point is the element in first column in first line, the second data point is the element in the second column in the first line element, the 11th data point is the element in the first column in the second line, and so on. Also keep in mind that the data first increment in x, then in y and finally in z. This means that if you split your scoring grid in N_x bins in x, N_y bins in y and N_z bins in z, the data points will be arranged in the file as following: the first N_x data points are the N_x x positions for the first y and the first z positions. The next N_x data points are the N_x x positions for the second y and the first z positions, and so on.

From the obtained datasets, you need to produce the following plots:

- 2D plots of the dose, for the measurements performed for determining the source center
- 1D plot of the dose, for the coarse longitudinal measurement, including errors
- 1D plot of the dose, for the fine longitudinal measurement, including errors and the $1/r^2$ fit
- 2D plots of the lateral dose measurements, for the 2 or 3 different depths
- 1D profiles through the center of the above mentioned 2D measurements
- 1D plot of the dose, for the fine longitudinal simulation, for the whole depth range
- 1D plot of the dose, for the fine longitudinal simulation, for the positive depth range, including the $1/r^2$ fit
- 2D plots of the lateral dose measurements, for the 2 or 3 different depths corresponding to your measurements
- 1D profiles through the center of the above mentioned 2D measurements

6.4. Contents of the Report

An important part to be evaluated in your lab course is the report. This has to be submitted by email, as a single PDF file. The report should contain the following sections.

A brief introduction to the experiment, the methods and the goals. This should contain some information on radioactivity and dose, and on the type of source you have used. You should also outline the goal of this experiment. You do not need to rewrite the complete manual.

After your introduction, you should add a section about the experiment. There you need to describe the experimental setup. Subsequently, you have to present step-by-step all the measurements you did, justify why you took these measurements, quote the results and interpret them. These are the calibration measurements, the source center measurements, the longitudinal and the lateral dose measurements. You will have to display in this section the plots mentioned above that are corresponding to the measured data. Also quote the $1/r^2$ fit parameters. Important points to discuss are any unsymmetries in the lateral profiles, the accuracy of the source center determination you made in the lab compared to what you get by fitting the data at home, the broadening of the lateral profiles with depth, the discrepancy between the $1/r^2$ fit and the data in the longitudinal profile.

The next part should be the simulation part. Briefly describe the simulation program and the parameters you utilized to run your simulations. Then, similarly to the measurements, you should present all the relevant plots of the simulations and quote the $1/r^2$ fit parameters. Finally, you have to interpret your results. Important points to discuss are any unsymmetries in the lateral profiles, the shape of the longitudinal profile at negative depth values, the effect of the voxel size, the broadening of the lateral profiles with depth, the discrepancy between the $1/r^2$ fit and the data in the longitudinal profile.

A necessary part of the report is the comparison of the experiment to the simulation. For that you need to present the 1D profiles of the longitudinal and of the lateral doses (extracted from the 2D at different depths). The comparison plots should contain the data normalized to the maximum (relative comparison) of each type dataset (measured, simulated), plotted in the same figure for each dataset type and using the same axes ranges. For example, the 1D measured and simulated longitudinal dose profile should be plotted in the **same** figure, with a horizontal axis range in mm or in cm and a vertical axis in normalized dose (maximum of 1). You should discuss the degree of agreement between these datasets. Also compare the fit parameters. Please note that at depth 0, the lateral profiles will not agree well. Try to explain why (it has to do with the real distance from the source and with the source size). Finally, you need to do one absolute dose comparison. After converting the longitudinal dose of the simulation to Gy/s, compare it in a single plot with the longitudinal dose from the measurement. Discuss the degree of agreement between the two.

You can close the report with a brief conclusion section.

Appendix A.

Inventory

A.1. General

- Workstation with EPSON 11000XL scanner[1] connected**??**, running WINDOWS

Figure A.1.: Scanning Workstation

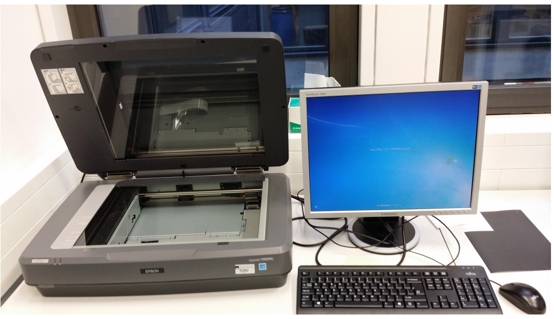

- Workstation with Optidos^{TM} and motor stage connected, running Windows.
- Water phantom

center

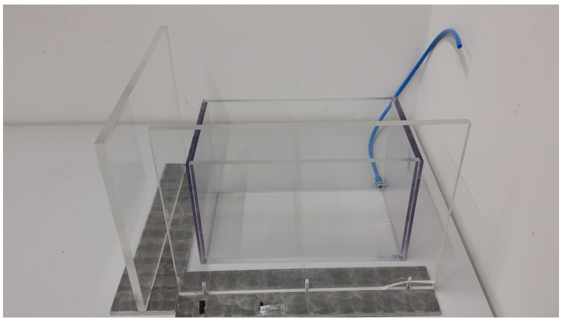

Figure A.2.: Water Phantom

- 2 acrylic walls
- Safe containing 2 beta-ray-sources of strontium-90 in their respective container

---

[1] please be very careful with it! The cost of this piece of hardware is in excess of 1500Â€

A.2. Gafchromic Films

- Sheet of gafchromic EBT-3-film, approximately 10 \cdot 12cm
- Scissors
- Marker pen
- Ruler
- Nitril gloves
- Box of Tissues
- Bottle of isopropyl alcohol
- Microfibre cloth
- Manual “Scanning gafchromic films”

A.3. Optidos^{TM}

- OPTIDOS-device
- Serial RS-232-Cable for connection to the Workstation (already installed)
- Optical fibre with scintillation detector attached
- “Kontrolladapter”
- 3-axis motor-stage (already connected to the workstation)
- Jerrycan of purified water (5l)
- Detector-mount
- Source-mount
- 2 screw drivers
- Several screws

Figure A.3.: Strontium90-source BL 730 in container mark 8921, view from top

Figure A.4.: Strontium-90-source BL 730 in container mark 8921

Figure A.5.: OPTIDOS-device

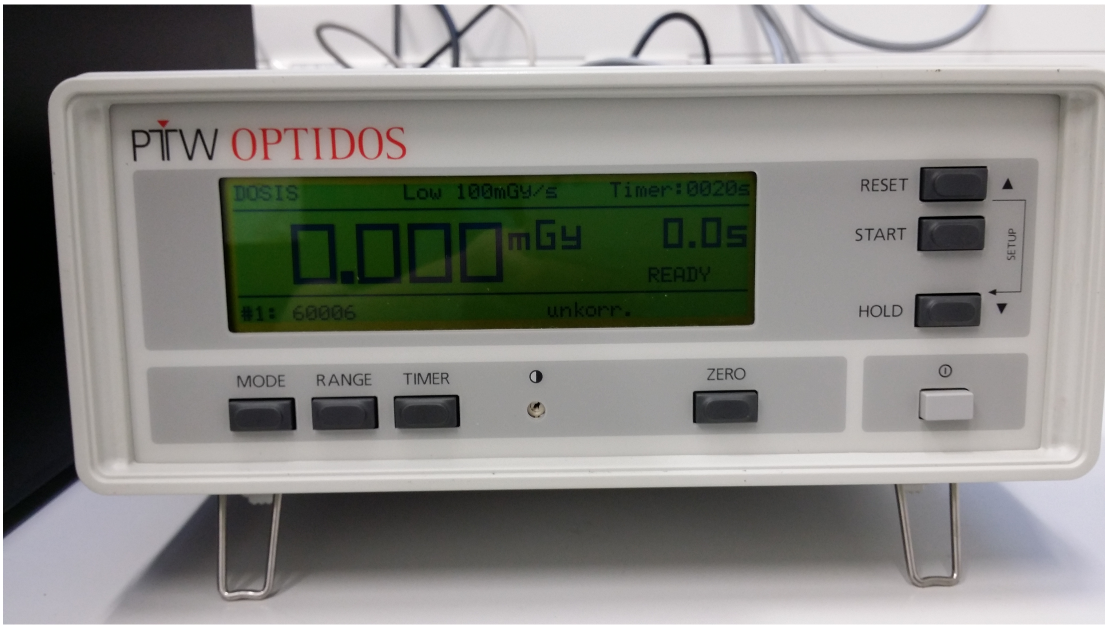

Appendix B.

Listings

List of Questions

List of Instructions

List of Algorithms

Appendix C.

Scanprotocol

Bibliography

[1] Nuclear medicine physics: a handbook for teachers and students.

[2] D Delacroix. *Radionuclide and radiation protection data handbook 2002*. Nuclear Technology Pub.

[3] Slobodan Devic, Jan Seuntjens, Edwin Sham, Ervin B. Podgorsak, C. Ross Schmidtlein, Assen S. Kirov, and Christopher G. Soares. Precise radiochromic film dosimetry using a flat-bed document scanner. 32(7):2245.

[4] Hanno Krieger. *Grundlagen der Strahlungsphysik und des Strahlenschutzes*. Vieweg+Teubner Verlag.